Effect of Fire on the Residual Mechanical Properties and Structural Performance of Reinforced Concrete Beams

JUI-HSIANG HSU*

Department of Civil Engineering, Ching Yun University
229 Chien-Hsin Rd., Jung-Li 320, Taiwan

CHERNG-SHING LIN

Department of Mechanical Engineering, Yuan Ze University
135 Yuan-Tung Rd., Jung-Li 320, Taiwan

ABSTRACT: This article relates to how fire affects residual mechanical properties and structural performance of reinforced concrete (RC) beams by combining thermal and structural analyses. Thermal analysis incorporates the finite difference method to model the temperature distribution in a RC beam subjected to heat transfer typical of that in a fire. Using the lumped method, structural analysis is performed to calculate the residual mechanical properties (bending moment, shear strength, and elastic modulus) of RC beams after fire exposure. As no two fires are the same, this novel scheme for predicting residual mechanical properties of fire-exposed RC beams is highly promising in that it eliminates the extensive testing otherwise required when determining fire ratings for structural assemblies.

KEY WORDS: fire effect on concrete, residual properties, RC beams and fire.

INTRODUCTION

FIRE IS A destructive force that causes thousands of deaths and significant property loss annually in Taiwan. People around the world expect that their homes and workplaces will be safe from the ravages of fire. Unfortunately, fire can occur in almost any building, often when least expected. More than 90% of the buildings in Taiwan are reinforced concrete (RC) structures. Moreover, Taiwan is located in a seismic belt region. Following fire damage, whether RC structures are sufficiently strong

*Author to whom correspondence should be addressed. E-mail: rhhsu@cyu.edu.tw

1042-3915/08/04 0245–30 $10.00/0 DOI: 10.1177/1042391507077171

SAGE Publications, Los Angeles, London, New Delhi and Singapore

enough (i.e., have sufficient residual strength) to withstand an earthquake must be determined to protect human life and property.

The fire safety of RC structures largely depends on their fire resistance, which mainly depends on the thermal conductivity and fire resistance of the main structural elements, i.e., beams and columns. Beams are subject to flexural and shearing loads. The residual bending moment and shear strength of fire-damaged RC beams are important factors in determining the safety of the RC structure. The effective elastic modulus also has a great influence in the deformation of RC beams exposed to fire. The study in this article combines thermal and structural analyses to model the residual bending moment, shear strength, and effective elastic modulus of RC beams after exposure to fire. These mechanical properties have different decreasing values during a fire. Modeling results help in understanding fire resistance and the deformation characteristics of RC beams exposed to fire.

The behavior of RC beams in fire conditions is governed by the properties of the constituent materials, concrete and steel, at high temperatures. Both concrete and steel undergo considerable changes in strength, stiffness, and other physical properties when subject to extreme heating. The modulus of elasticity decreases as temperature increases [1]. Numerous studies have investigated the effects of fire on concrete [2–4], and steel [2,4–6].

Analyzing the mechanical properties of RC elements after exposure to high temperatures for long periods requires that the temperature distribution in cross sections are known. This distribution is obtained from thermal analysis using the thermal properties of the materials, including heat capacity and thermal conductivity. The study in this article models temperature distributions of rectangular concrete beams maintained at high temperatures. Modeling results compared to existing data achieved reasonable agreement with the isothermal contours obtained by Lin [7], who analyzed the temperature distribution in pure concrete beams heated according to the time–temperature curve for a standard fire.

The increase in ambient temperature changes the temperature distribution inside a beam's cross sections. After exposure to high temperatures, the mechanical properties of reinforcing steel and concrete vary according to the fire-induced temperatures. This makes the stress distribution in such beam structures difficult to determine.

Structural analysis in the proposed model complies with the American Concrete Institute (ACI) building codes, which consider how temperature affects reinforcing steel and concrete using a lumped system approach to determine the residual bending moment, shear strength, and elastic modulus. Modeling results for bending moments were compared with calculated results using the ACI codes at room temperature and with full-scale RC beam fire exposure experiments [8,9]. The residual shear

strength, and effective elastic modulus derived analytically were also compared with data obtained by other studies [8,10]. The consistency between modeling and experimental results confirmed the accuracy of the proposed model.

TEMPERATURE ANALYSIS

In a real fire or a fire test, heat will flow to the surface of the structure exposed to fire by means of radiation and convection. The heat will then be transferred internally away from the surface by means of conduction. Because of the time dependency of the gas temperature, this heat transfer is classified as a 'transient' temperature analysis problem.

Accurately predicting the temperature variation within the structural element with time is essential for determining the corresponding material properties at the relevant temperatures, and carrying out the structural analysis. The Finite Difference Method is used in the temperature distribution analysis. The fundamental equation that represents transient heat conduction in a solid under the continuity condition is typically presented in its well-known differential form,

$$\gamma(T)c(T)\frac{\partial T}{\partial t} + \nabla \cdot q'' = u'''. \tag{1}$$

The density of concrete $\gamma(T)$ depends on the aggregate and mixture design (see the Nomenclature list at the end of this article for a definition of all symbols). Typical 'dense' concrete has a density of $\sim$2300 kg/m^3. When concrete is heated to 100°C, density usually decreases by up to 100 kg/m^3 due to the evaporation of free water, which has a minor effect on thermal response. Besides moisture changes, the density of concrete does not change much at elevated temperature, except for calcareous aggregate concrete, which decomposes at $\sim$800°C with a corresponding sudden decrease in density [11]. In the current model, the density of concrete is assumed to be the constant value of 2300 kg/m^3. The specific heat $c(T)$ of concrete for anorthosite and expanded shale aggregates, calculated by Harmathy [12], increases smoothly from 0.71 kJ/kg K at 25°C to 1.22 kJ/kg K at 1000°C.

STRUCTURAL ANALYSIS

The study in this article considers the fire-related factors that affect reinforcement bars and concrete materials, using the lumped system approach, and determines the residual bending moment, shear strength, and effective elastic modulus of RC beams following fire damage.

The lumped system concept is taken from thermal conduction models. When heat is transferred through a medium, the temperature varies with time and position. Under certain conditions, temperature varies only linearly with time; such a system is called a Lumped System [13]. The concept underlying the original lumped system is extended in the sense that material temperature and mechanical characteristics are respectively considered to be invariant with position. The temperature and mechanical properties of a unit are assumed to be the same as those at the unit center. In this study, the unit mesh is 10 mm × 10 mm. Modeling results reveal that using a smaller mesh to calculate the residual bending moment, shear strength, and effective elastic modulus of RC beams exposed to fire only result in changes of <1%.

Residual Bending Moment of Reinforced Concrete Beams Exposed to Fire

A beam is defined as a structural member predominantly subject to bending moment. The ultimate bending moment of a beam is its flexure before failure occurs. The ACI code [14] provides a general expression for the balanced state that links the tensile strength of reinforcing steels, compressive strength of concrete, their respective moduli, and the reinforcement ratio ρ. The balanced steel ratio ρ_b, is determined by identifying the reinforcement ratio of a balanced condition in which failure would occur simultaneously in the concrete and reinforcing steels. In order to ensure yielding of steel before crushing of concrete, the codes provisions are intended to ensure a ductile mode of failure by limiting the amount of tension reinforcement ratio ρ_{max}, to 75% of ρ_b. On the other hand, the flexural failure in the case of RC beams with a very small amount of tensile reinforcement can be sudden. A minimum amount of tensile reinforcement ratio ρ_{min}, is required to prevent such failure.

Equilibrium should exist between the compressive force (C_{om}) and tensile force (T_{en}) acting on a beam cross section at a nominal strength when the beam is computed by the strength design method in the code. For rectangular sections of beams with tension reinforcement only, equilibrium conditions are as follows:

Force equilibrium:

$$\begin{aligned} C_{om} &= T_{en} \\ 0.85 f_c' ab &= A_s f_y = \rho b d f_y \\ a &= \frac{A_s f_y}{0.85 f_c' b} = \frac{\rho d f_y}{0.85 f_c'}. \end{aligned} \tag{2}$$

Moment equilibrium:

$$M_n = (C_{\text{om}} \text{ or } T_{\text{en}})\left[d - \frac{a}{2}\right] = \rho b d f_y \left[d - \frac{0.5\rho d f_y}{0.85 f'_c}\right]. \tag{3}$$

The stress-related strain includes the elastic and plastic components of strain resulting from applied stress. The stress–strain relationships for concrete at elevated temperatures have been simplified and redrawn (Figure 1) according to Eurcode 2 (EC2) [15]. From the stress–strain relationships for concrete at elevated temperatures, the stress–strain relationship of concrete is a function of temperature [11]. The residual compressive stress and elastic modulus of concrete after exposure to high temperatures decline as temperature increases. The residual compressive stress of concrete under sustained elevated temperature can thus be retrieved for a given temperature and strain.

In the study in this article, the cross section of an RC beam is divided into $M \times N$ segments for analysis. Each segment assumed to have a uniform (but different from other elements) temperature and iso-properties, according to the lumped system concept. A computer program was developed to calculate

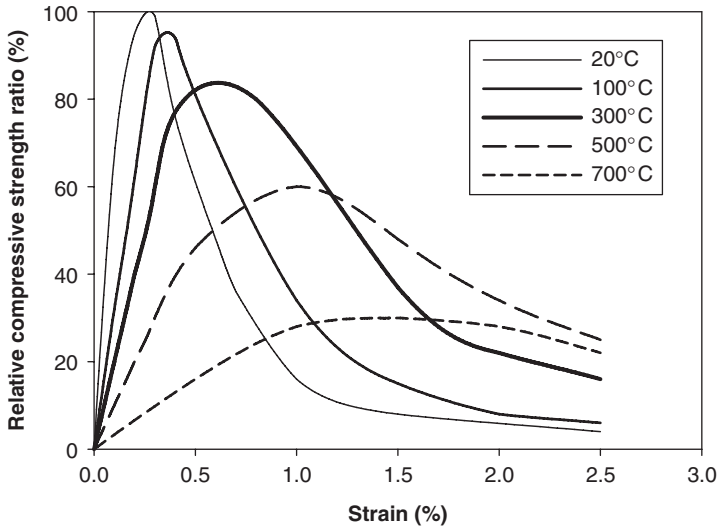

Figure 1. *Stress–strain relationships for concrete at elevated temperature (simplified and redrawn according to EC2 [15]).*

the residual bending moment of RC beams after exposure to fire. Figure 2 presents the calculation flow chart of the program.

The critical concrete compressive strain that crushes the beam is first assumed to be ε_{cp}. The distance from the extreme compression fiber to the neutral axis c, is then defined. Combining the temperature distribution of the cross section calculated from the thermal model and the strain, a residual compressive stress matrix can be obtained from the stress–strain relationships in [15] (Figure 1).

According to the assumption in the ACI code [14], the tensile strength of the concrete is neglected in calculating the bending moment. The tensile force of the cross sections of RC beams can be derived by,

$$T_{\text{en}} = A_s \cdot f_{yr}. \tag{4}$$

The reduction in yield strength of steel is defined by a number of points. Eurcode 3 (EC3) [16] gives an expression of the approximate curve for the reduction in yield strength of steel.

$$k_{y,T} = \left[0.9674\left(1 + \exp\left[\frac{(T - 482)}{39.19}\right]\right)\right]^{-1/3.833}. \tag{5}$$

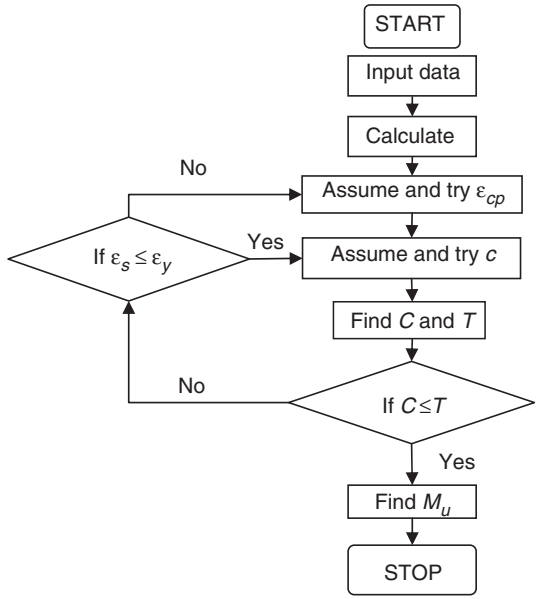

Figure 2. *Flowchart for calculated residual flexural capacity of RC beam exposed to fire.*

The compressive strength of the cross section of RC beams can be calculated by summing all the compressive strengths on the compressive side of the lumped units.

$$C_{\text{om}} = \sum_{i=1}^{M} \sum_{j=1}^{c/\Delta y} f_{c,ij}^{T} \cdot \Delta x \cdot \Delta y. \tag{6}$$

If the sectional stress of the cross section is in static equilibrium, Equations (4) and (6) should be equal. If not, the assumed c value is likely too small to satisfy the equilibrium. In this case, the c value is increased and the calculation is repeated. When the equilibrium remains unsatisfactory after adjusting the c value, it is assumed that ε_{cp} is too small and ε_{cp} is increased. This process continues until Equations (4) and (6) are equal.

When the beam cross section is in static equilibrium, the residual ultimate moment of the beam M_u can be calculated as

$$M_u = A_s \cdot f_{yr} \cdot \left(d - \frac{\sum_{i=1}^{M} \sum_{j=1}^{c/\Delta y} f_{c,ij}^{T} \cdot \Delta x \cdot \Delta y \cdot j \cdot \Delta y}{\sum_{i=1}^{M} \sum_{j=1}^{c/\Delta y} f_{c,ij}^{T} \cdot \Delta x \cdot \Delta y} \right) \tag{7}$$

Thermal Stress Distribution of Reinforced Concrete Beams Exposed to Fire

Because of the fact that different parts of the beam cross section are exposed to different temperatures during a fire, the stress distribution in such beam structures is a significant problem. This study simulates the thermal stress distribution in the cross-section under different torque loads.

Figure 3 plots the simulated thermal stress distributions in a 300 mm wide cross section, an effective depth of 450 mm with 3 ϕ 25 mm (where 3 ϕ 25 mm means 3 steel rebar, each with a diameter of 25 mm) as the main reinforcing bar under torque loadings of 50 kN m and 200 kN m after 2.5 hours of heating on three surfaces using the standard temperature-rise curve. The ratio of the compressive stress of the concrete to the tensile stress of the steel bar in the Figure 3 is 1/20.

The stress distribution on both sides of the concrete above the neutral axis is significantly reduced by exposure to high temperatures. The factor most strongly influencing the central part is the stress–strain relationship, as temperature has a weak effect on the central part. Under a small bending moment (50 kN m), the stress–strain relationship for the central part is elastic; when the bending moment increases (200 kN m), the stress–strain relationship is generally plastic.

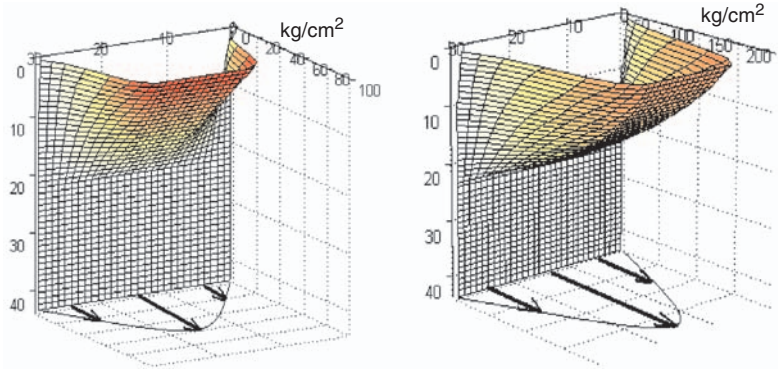

Figure 3. *Thermal stress distribution under different torque loads after 2.5 hours of fire exposure.*

Residual Shear Strength of Reinforced Concrete Beams Exposed to Fire

The shear strength is based on an average shear stress on the full effective cross section. In a member with shear reinforcement, a portion of the shear strength is assumed to be provided by the concrete and the remainder by the shear reinforcement. According to the ACI code [14], the nominal shear strength of an RC beam can be determined as,

$$V_n = V_c + V_s. \tag{8}$$

For normal beams ($l_n/d > 5$) subject to shear and flexure only, (The formulas are transformed to SI units)

$$V_c = \left(0.50\sqrt{f'_c} + 176\rho\frac{V_u d}{M_u}\right)bd \le 0.93\sqrt{f'_c}bd \tag{9}$$

$$V_s = \frac{A_v f_y d}{s}. \tag{10}$$

For deep beams ($l_n/d < 5$), (The formulas are transformed to SI units)

$$V_c = \left(3.5 - 2.5\frac{M_u}{V_u d}\right)\left(0.50\sqrt{f'_c} + 176\rho\frac{V_u d}{M_u}\right)bd \le 1.59\sqrt{f'_c}bd \tag{11}$$

$$V_s = \frac{A_v f_y d}{s}\left(\frac{1 + L_n/d}{12}\right) + \frac{A_{vh} f_y d}{s_h}\left(\frac{11 - L_n/d}{12}\right). \tag{12}$$

Based on ACI code assumptions [14] and the effects of temperature, the cross section is divided into $M \times N$ segments. Each segment can exhibit a

uniform temperature and iso-properties. The shear strength of the RC beam cross section can be determined by summing the shear strengths of all of the lumped units. A computer program sums the residual strengths for all lumped units, as in Equations (13)–(18).

$$V_{rn} = V_{rc} + V_{rs}. \tag{13}$$

For normal beams, $(l_n/d > 5)$

$$\begin{aligned} V_{rc} &= \sum_{i=1}^{n}\sum_{j=1}^{m} V_{rc,ij} = V_{rc,11} + V_{rc,12} + \cdots + V_{rc,21} + V_{rc,22} \\ &\quad + \cdots + V_{rc,n1} + V_{rc,n2} + \cdots V_{rc,nm} \\ &= \sum_{i=1}^{n}\sum_{j=1}^{m}\left(0.50\sqrt{f'_{cr,ij}} + 176\rho\frac{V_u d}{M_u}\right)A_{ij} \\ &\le \sum_{i=1}^{n} 0.93\sqrt{f'_{cr,ij}}A_{ij}, \quad \hat{S}\hat{Z}\frac{V_u d}{M_u} \le 1 \end{aligned} \tag{14}$$

$$V_{rs} = \frac{A_v f_{yr} d}{s} \tag{15}$$

where, the subscript r is the residual value of the properties after the unit sustains a high temperature, and f'_{cr} is the residual compressive strength of the concrete after heating. Experimental data obtained by Abrams [17] are used to derive a conservative formula for residual compressive strength of concrete exposed to high temperatures:

$$f'_{cr} = \begin{cases} (1 - 0.001T)f'_c & 0^{\circ}\mathrm{C} \le T \le 500^{\circ}\mathrm{C} \\ (1.375 - 0.00175T)f'_c & 500^{\circ}\mathrm{C} \le T \le 700^{\circ}\mathrm{C} \\ 0 & 700^{\circ}\mathrm{C} \le T \end{cases} \tag{16}$$

For deep beams, $(l_n/d < 5)$

$$\begin{aligned} V_{rc} &= \sum_{i=1}^{n}\sum_{j=1}^{m} V_{rc,ij} = V_{rc,11} + V_{rc,12} + \cdots + V_{rc,21} + V_{rc,22} \\ &\quad + \cdots + V_{rc,n1} + V_{rc,n2} + \cdots V_{rc,nm} \\ &= \sum_{i=1}^{n}\sum_{j=1}^{m}\left(3.5 - 2.5\frac{M_u}{V_u d}\right)\left(0.50\sqrt{f'_{cr,ij}} + 176\rho\frac{V_u d}{M_u}\mathrm{e}\right)A_{ij} \\ &\le \sum_{i=1}^{n}\sum_{j=1}^{m} 1.59\sqrt{f'_{cr,ij}}A_{ij}, \quad \hat{S}\hat{Z}\left(3.5 - 2.5\frac{M_u}{V_u d}\right) \le 2.5 \end{aligned} \tag{17}$$

$$V_{rs} = \frac{A_v f_{ry} d}{s}\left(\frac{1 + L_n/d}{12}\right) + \frac{A_{vh} f_{ry} d}{s_h}\left(\frac{11 - L_n/d}{12}\right). \tag{18}$$

Effective Elastic Modulus of Reinforced Concrete Beams Exposed to Fire

Reinforced concrete beams are made of concrete and reinforcing steels. The analysis of the behavior of RC beams under flexure usually transforms the section of steel to n times that of the concrete, $n = E_s/E_c$, which is known as the modular ratio, in the so-called 'transformed section method'. After sustaining high temperature, the mechanical properties of reinforcing steel and concrete vary according to the fire-induced temperature. It makes the effective elastic modulus in such beam structures difficult to determine. In the study, in this article, an RC beam cross section is divided into $M \times N$ segments for analysis. Based on the lumped system concept, each segment is considered to have a uniform (but different from other elements) temperature and iso-properties. The approximate engineering formulas for determining the effective elastic modulus of a RC beam is obtained using the interface layer approach [18].

The effects of temperature on the elastic modulus of concrete and the reinforcing bars must be known to model the effective elastic modulus of RC beams exposed to fire. Reduction in the modulus of elasticity of the reinforcing bars with temperature is specified by [16]

$$\begin{aligned} k_{E.T} &= 1.0 + T/\left[2000 \ln\left(\frac{T}{1100}\right)\right] \qquad 0 < T \leq 600^{\circ}\mathrm{C} \\ &= \frac{690(1 - T/1000)}{(T - 53.5)} \qquad 600^{\circ}\mathrm{C} < T \leq 1000^{\circ}\mathrm{C}. \end{aligned} \tag{19}$$

The modulus of elasticity of concrete also decreases as the temperature increases. The reduction ratio given in EC2 [15] is,

$$\begin{aligned} k_{E.T} &= 1.0 \qquad \text{for } T < 150^{\circ}\mathrm{C} \\ k_{E.T} &= \frac{(700 - T)}{550} \quad \text{for } T > 150^{\circ}\mathrm{C}. \end{aligned} \tag{20}$$

For a given beam (Figure 4), the effective elastic modulus of every horizontal strip (each with M parallel strips) was determined first. According to the interface layer approach [18], parallel strips are formulated with various e_{ij} values, as presented in Figure 5. The effective elastic

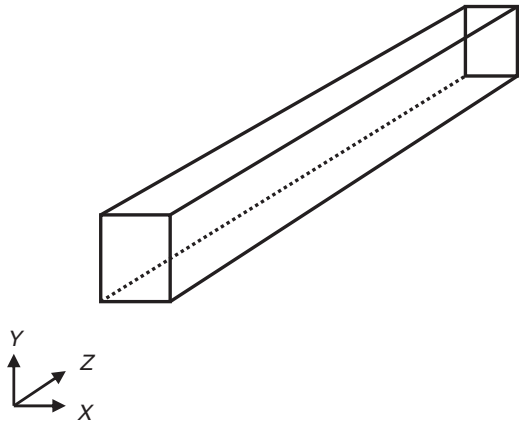

Figure 4. *Beam coordinates.*

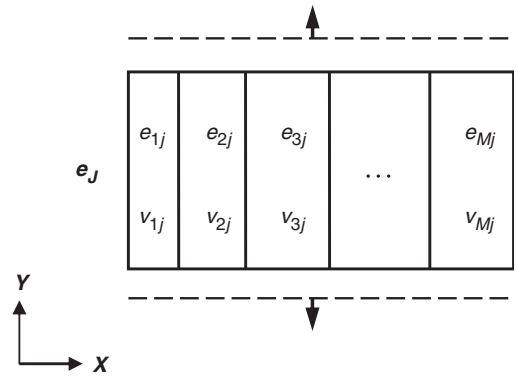

Figure 5. *Horizontal strip J (with different parallel elastic moduli).*

modulus e_J of the combined body is obtained from the compatibility of their longitudinal deformations under loading (each strip has a different stress). The effective elastic modulus of a horizontal strip J can be formulated as,

$$e_J = \sum_{i=1}^{M} e_{ij} \frac{v_{ij}}{\sum_{i=1}^{M} v_{ij}} = e_{1j} \frac{v_{1j}}{v_{1j} + v_{2j} + v_{3j} + \cdots} + e_{2j} \frac{v_{2j}}{v_{j1} + v_{2j} + v_{3j} + \cdots} + \cdots \tag{21}$$

where, e_{ij} and v_{ij} $(i = 1, 2, 3, \ldots)$ are the elastic modulus and volume of each parallel strip in the horizontal strip J, respectively.

For horizontal strips with various e_J values (Figure 6), let each strip be subject to the same stress during deformation. The vertical displacement of each strip is taken as the weighted average of the vertical displacement of each part of the strip. Then, to add the vertical displacement of each strip we obtain the total vertical displacement of the model from which we may obtain an effective elastic modulus E_e for this combined body (each strip has a different deformation).

$$E_e = \frac{1}{\sum_{J=1}^{N} V_J/e_J \sum_{J=1}^{N} V_J} = \frac{1}{V_1/e_1(V_1+V_2+V_3+\cdots)+V_2/e_2(V_1+V_2+V_3+\cdots)+\cdots} \tag{22}$$

where, e_J and V_J $(J=1,\ 2,\ 3,\ldots)$ are the effective elastic modulus and volume of each of the horizontal strips, respectively, and E_e is the effective elastic modulus of the beam.

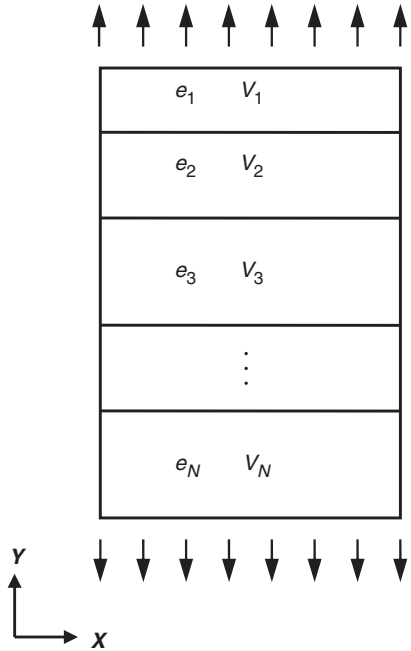

Figure 6. *Parallel strip (with different horizontal elastic moduli).*

VALIDATION AGAINST EXPERIMENTAL RESULTS

Validation of Ultimate Moment

Lin [7] investigated the temperature distribution of pure concrete materials during a fire. For convenience of comparison, the dimensions 304.8 mm × 416.4 mm (12 × 16 in.), which were used by Lin [7] are assumed here to simulate the temperature distribution of the beam cross section of which three surfaces (the top was insulated) were exposed to the American Society for Testing and Materials (ASTM) E 119 standard temperature-rise curve [19]. Figure 7 plots the comparison of results with isothermal contours. A very close match exists between isotherms during the 2 hours of fire, and a similar match exists between isotherms following 3 hours of fire, with the exception of a small deviation at 500–600°C.

At room temperature (20°C), the ultimate bending moment M_u is calculated for beam cross sections of 200 mm × 400 mm, 300 mm × 450 mm, and 300 mm × 600 mm with three steel ratios of $\rho_{\min}$, $\rho_{\max}$, and $1/2(\rho_{\max} + \rho_{\min})$, given $\text{fc}' = 2.06 \times 10^7$ Pa and $\text{fy} = 4.12 \times 10^8$ Pa. Table 1 presents the computational results of ultimate bending moments from the ACI code and those obtained from this study. Figure 8 presents a diagrammatic comparison of study and code results (Table 1). The code and modeled residual bending moments for typical dimensions are in good agreement, as determined by comparing the calculations for the nonfire situation with ACI code data.

The residual ultimate bending moment of an RC beam exposed to fire is verified by Moetaz et al. [8] and Ho [9]. Moetaz et al. [8] fabricated four reinforced beams, each 200 mm deep, 120 mm wide and 1800 mm long. The beams were reinforced with 2 $\oint$ 10 mm steel as the main reinforcement, 2 $\oint$ 10 mm steel as the secondary reinforcement, and $\oint$ 8 mm steel as stirrups with 80 mm spacing. The beams were installed in the fire test chamber 40 days after casting. During fire testing, the unloaded beams were exposed to fire at 650°C (Figure 9). The chamber was controlled so that the same average temperature–time curve was followed for all beams. Beams were exposed to fire for 30, 60, and 120 minutes and the control beam was not exposed to fire. After cooling to room temperature, the beams were tested to failure by applying two increasing transverse loads (Figure 10). Table 2 presents the test and modeling results for beams (B, B_1, B_2, and B_3) exposed to fire for 0, 30, 60, and 120 minutes, respectively. Figure 11 compares diagrammatically the residual bending moment obtained between experimental and modeling results. For beam B3 (exposed to fire for 120 minutes), the mathematical expressions overestimate the bending strength of the experimental result, indicating that long-term fire damage

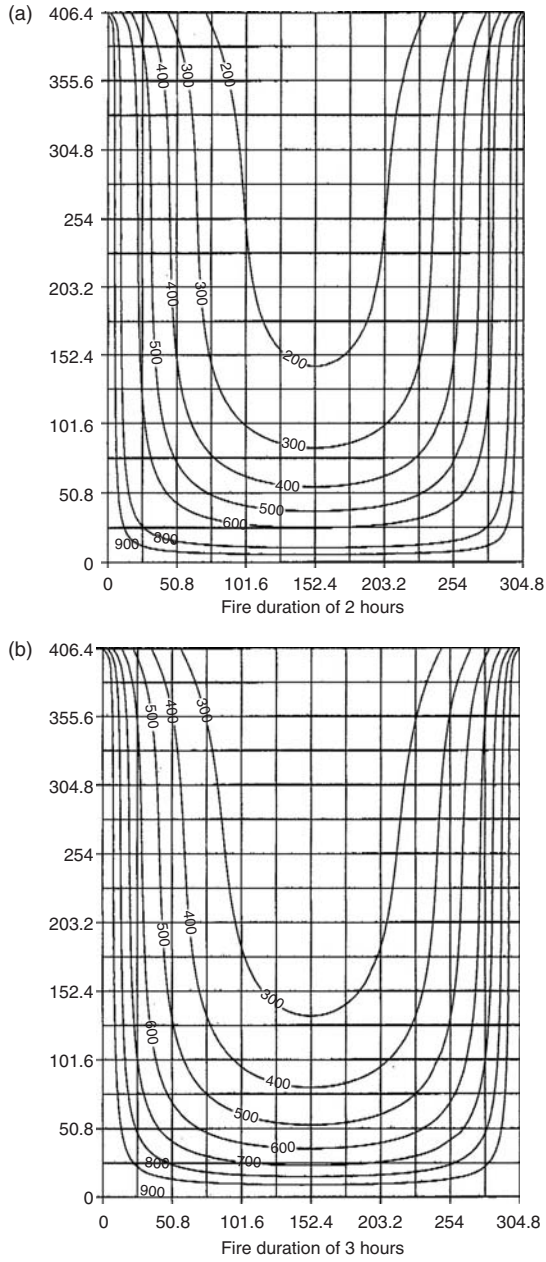

Figure 7. *Comparison of isothermal contours in concrete beams during fire exposure.*

Table 1. Ultimate bending moment (kN m) from ACI Code and modeling for various beam section and reinforcing ratios at room temperature.

	200 mm × 400 mm		300 mm × 450 mm		300 mm × 600 mm	
Reinforcing ratio	**Code**	**Modeling**	**Code**	**Modeling**	**Code**	**Modeling**
ρ_{min}	42.18	42.18	80.15	80.05	142.34	142.44
$1/2(\rho_{max} + \rho_{min})$	127.43	128.51	241.91	243.97	429.97	434.39
ρ_{max}	193.75	196.79	367.97	373.66	654.03	664.92

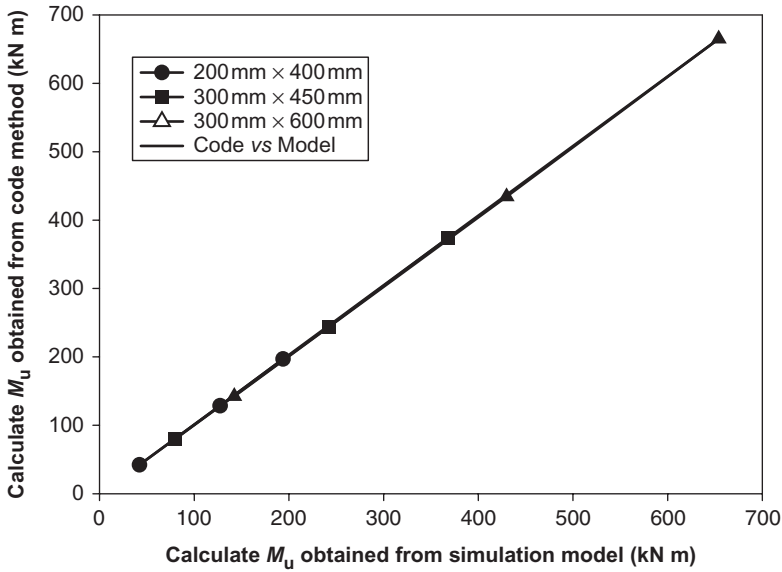

Figure 8. *Comparison of ultimate bending moment (M_u) obtained from the ACI Code method and simulated results for various dimensions of beams and steel ratios.*

may have destroyed the beam structure. The predicted residual bending moment of beams exposed to fire for a relatively long period typically exceed actual values, so the proposed model should be applied conservatively in such cases.

The residual ultimate bending moment of an RC beam exposed to fire was also verified by Ho [9]. Ho [9] manufactured 300 mm × 500 mm × 3400 mm full-scale RC beams. The beams were reinforced with 2 ϕ 22 mm as the main reinforcement on the compressive side, 2 ϕ 25 mm (outer side) and 2 ϕ 22 mm (inner side) as the main reinforcements on the tensile side, and ϕ 10 mm steel as the stirrup. All investigated beams were cured under the same conditions

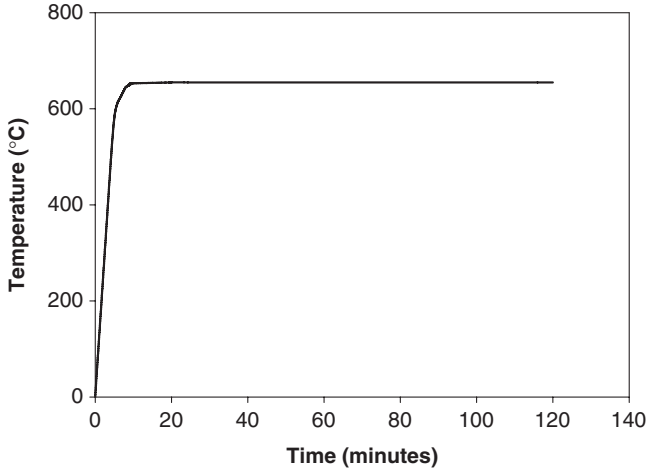

Figure 9. *Time–temperature curve.*

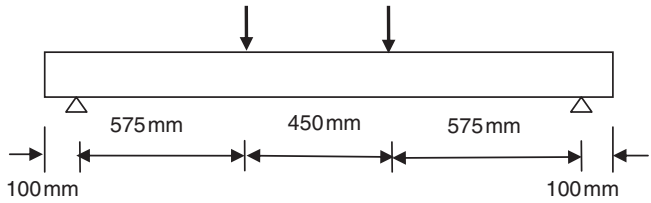

Figure 10. *Fire flexural test conditions.*

Table 2. Ultimate bending moment from experiment and modeling for beams exposed to fire.

	Beams			
Properties	**B**	**B1**	**B2**	**B3**
Fire exposure time (minutes)	0	30	60	120
Ultimate loads from test (*t*)	5.95	5.25	4.80	3.65
Ultimate bending moment from experiment (kN m)[a]	16.78	14.81	13.54	10.50
Ultimate bending moment from modeling (kN m)	15.25	13.76	13.09	11.82

[a]Calculation from test ultimate loads as the loading in Figure 10.

inside the laboratory and then positioned in a gas furnace; the beams were heated according to the ASTM E119 standard temperature-rise curve through three surfaces. The beams were insulated on their top surfaces. After natural cooling, the beams were loaded and tested to fracture.

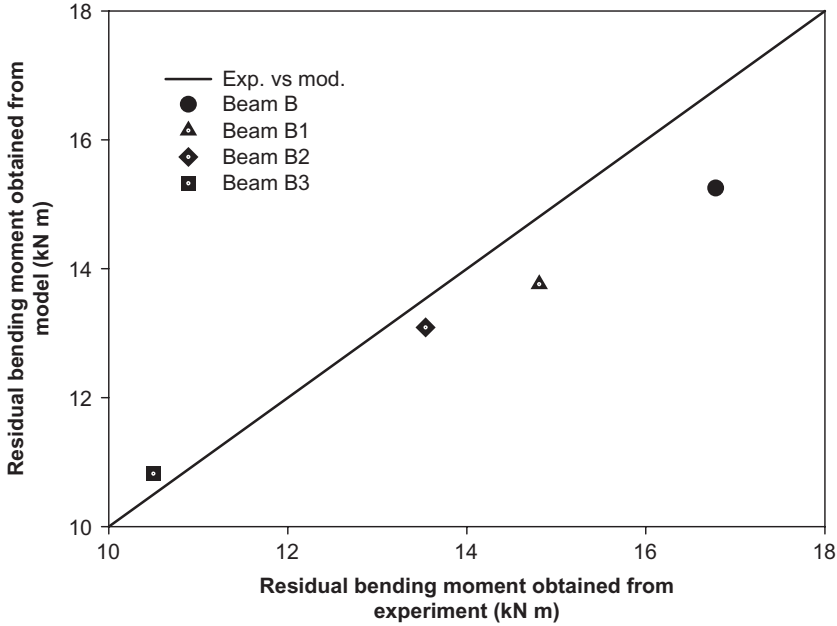

Figure 11. *Comparison of residual bending moments obtained from experimental and modeling results.*

Table 3. Ultimate bending moment from experiment and modeling for beams exposed to fire.

	Experiment data (kN m)	Modeling data (kN m)
0	279.00	273.64
2.5 hours	252.31	217.09
3.5 hours	228.77	201.16

Three beams (N3B2, B3B2, and D3B2) were tested to determine the residual ultimate bending moments after heating for 0, 2.5, and 3.5 hours, respectively. Table 3 presents the test and modeling results. Figure 12 diagrammatically compares the residual ultimate bending moment for experimental and modeling results in Table 3. The calculated values are slightly lower than the experimental values, meaning the calculation is conservative (Figure 12). Agreement between the experimental (code) and modeling results (Figures 8, 11, and 12) show that using the proposed calculation procedure in this study is suitable.

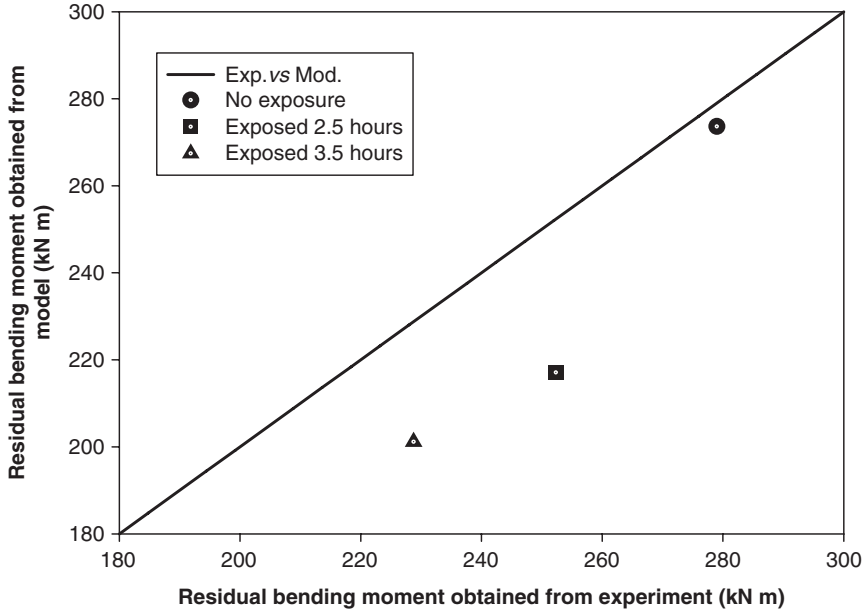

Figure 12. *Comparison of residual bending moments obtained from experimental and modeling results.*

Validation of Shear Strength

Lin et al. [10] fabricated 35 full-scale RC beams (Table 4) with various dimensions and parameters. All beams were cured under the same conditions in a laboratory. After curing for 28 days, the beams were placed in a gas furnace. The beams were heated according to the ASTM E 119 standard temperature-rise curve [19] through three surfaces; beam tops were insulated. After natural cooling, the beams were loaded using the two-point method and tested to failure. Table 5 presents experimental and simulated data for residual shear force of the beams. The calculated and experimental data follow similar trends (Figure 13). The calculated values are typically less than experimental values, indicating that results are conservative.

Validation of Modulus of Elasticity

The study in this article implemented the experimental program in [8] and added the boundary temperature–time curve into the temperature distribution simulation in the last section. The temperature of each segment in the

Table 4. Full-scale RC Beams.

Test no.	Sample size (m)	Ln/*d*	*a*/*d*	*b* (m)	*d* (m)	f'_c (kg/m^2)	Tensile steel	Stirrup	Duration of fire (hours)
1	0.2 × 0.3 × 1.6	4.54	1.5	0.2	0.26	3.47E6	3 ϕ 22 mm	0	0
2	0.2 × 0.3 × 1.6	4.54	1.5	0.2	0.26	3.47E6	3 ϕ 22 mm	0	1
3	0.2 × 0.3 × 1.6	4.54	1.5	0.2	0.26	3.47E6	3 ϕ 22 mm	0	3
4	0.2 × 0.3 × 3.0	9.54	4.0	0.2	0.26	3.47E6	3 ϕ 22 mm	0	0
5	0.2 × 0.3 × 3.0	9.54	4.0	0.2	0.26	3.47E6	3 ϕ 22 mm	0	1
6	0.2 × 0.3 × 3.0	9.54	4.0	0.2	0.26	3.47E6	3 ϕ 22 mm	0	3
7	0.2 × 0.3 × 1.6	4.67	1.5	0.2	0.24	3.58E6	6 ϕ 22 mm	0	0
8	0.2 × 0.3 × 1.6	4.67	1.5	0.2	0.24	3.58E6	6 ϕ 22 mm	0	1
9	0.2 × 0.3 × 1.6	4.67	1.5	0.2	0.24	3.58E6	6 ϕ 22 mm	0	3
10	0.2 × 0.3 × 3.0	9.67	4.0	0.2	0.24	3.58E6	6 ϕ 22 mm	0	0
11	0.2 × 0.3 × 3.0	9.67	4.0	0.2	0.24	3.58E6	6 ϕ 22 mm	0	1
12	0.2 × 0.3 × 3.0	9.67	4.0	0.2	0.24	3.58E6	6 ϕ 22 mm	0	3
13	0.2 × 0.3 × 1.6	4.54	1.5	0.2	0.26	3.47E6	3 ϕ 22 mm	ϕ 10 mm@ 80 mm	0
14	0.2 × 0.3 × 1.6	4.54	1.5	0.2	0.26	3.47E6	3 ϕ 22 mm	ϕ 10 mm@ 80 mm	1
15	0.2 × 0.3 × 1.6	4.54	1.5	0.2	0.26	3.47E6	3 ϕ 22 mm	ϕ 10 mm@ 80 mm	3
16	0.3 × 0.45 × 2.0	4.11	1.5	0.3	0.36	3.47E6	6 ϕ 22 mm	0	0
17	0.3 × 0.45 × 2.0	4.11	1.5	0.3	0.36	3.47E6	6 ϕ 22 mm	0	1
18	0.3 × 0.45 × 2.0	4.11	1.5	0.3	0.36	3.47E6	6 ϕ 22 mm	0	3
19	0.3 × 0.45 × 2.7	9.11	4.0	0.3	0.36	3.58E6	8 ϕ 28 mm	0	0
20	0.3 × 0.45 × 2.7	9.11	4.0	0.3	0.36	3.58E6	8 ϕ 28 mm	0	1
21	0.3 × 0.45 × 2.7	9.11	4.0	0.3	0.36	3.58E6	8 ϕ 28 mm	0	3
22	0.3 × 0.45 × 2.0	4.11	1.5	0.3	0.36	3.47E6	6 ϕ 22 mm	ϕ 10 mm@ 80 mm	0
23	0.3 × 0.45 × 2.0	4.11	1.5	0.3	0.36	3.47E6	6 ϕ 22 mm	ϕ 10 mm@ 80 mm	3
24	0.3 × 0.45 × 3.7	9.11	4.0	0.3	0.36	3.58E6	8 ϕ 28 mm	ϕ 10 mm@ 150 mm	0
25	0.3 × 0.45 × 3.7	9.11	4.0	0.3	0.36	3.58E6	8 ϕ 28 mm	ϕ 10 mm@ 150 mm	3
26	0.2 × 0.3 × 1.6	4.54	1.5	0.2	0.26	5.98E6	3 ϕ 22 mm	0	0
27	0.2 × 0.3 × 1.6	4.54	1.5	0.2	0.26	6.05E6	3 ϕ 22 mm	0	1
28	0.2 × 0.3 × 1.6	4.54	1.5	0.2	0.26	6.25E6	3 ϕ 22 mm	0	3
29	0.2 × 0.3 × 3.0	9.54	4.0	0.2	0.260.26	6.01E6	3 ϕ 22 mm	0	0
30	0.2 × 0.3 × 3.0	9.54	4.0	0.2	0.26	7.16E6	3 ϕ 22 mm	0	1
31	0.2 × 0.3 × 1.6	4.67	1.5	0.2	0.24	6.34E6	6 ϕ 22 mm	0	0
32	0.2 × 0.3 × 1.6	4.67	1.5	0.2	0.24	6.52E6	6 ϕ 22 mm	0	1
33	0.2 × 0.3 × 1.6	4.67	1.5	0.2	0.24	6.65E6	6 ϕ 22 mm	0	3
34	0.2 × 0.3 × 3.0	9.67	4.0	0.2	0.24	6.09E6	6 ϕ 22 mm	0	0
35	0.2 × 0.3 × 3.0	9.67	4.0	0.2	0.24	6.57E6	6 ϕ 22 mm	0	1

Table 5. Comparisons of experimental data with simulated data on residual shear strength.

Test no.	Experimental data (kN)	Simulated data (kN)	Test no.	Experimental data (kN)	Simulated data (kN)
1	177.56	132.53	19	138.81	122.57
2	213.86	104.77	20	211.90	104.95
3	188.84	79.66	21	117.23	89.17
4	63.57	52.48	22	471.66	389.33
5	48.76	43.75	23	467.64	310.08
6	57.68	27.27	24	375.04	250.87
7	276.15	177.36	25	311086	217.48
8	320.98	149.11	26	283.71	161.28
9	220.72	123.61	27	337.46	124.36
10	79.85	54.57	28	229.46	92.01
11	89.17	48.33	29	89.27	67.54
12	41.30	32.65	30	89.76	59.18
13	289.89	212.35	31	466.96	207.30
14	270.56	184.56	32	471.37	170.89
15	243.09	159.45	33	246.53	136.98
16	431.84	287.33	34	123.21	68.13
17	468.33	244.39	35	130.28	61.91
18	279.00	208.09			

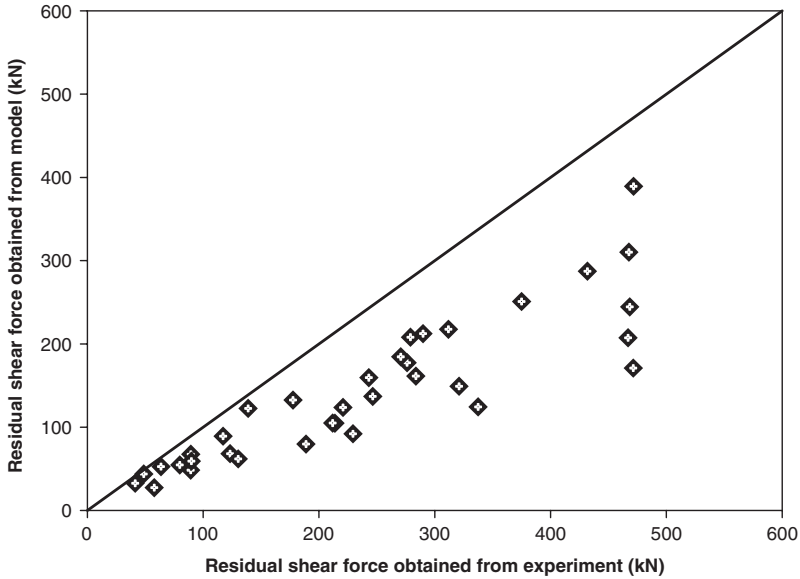

Figure 13. *Comparison of residual shear forces obtained from experimental and modeling results.*

section of the RC beams was obtained. Equation (22) yields the effective elastic modulus of RC beams exposed to fire. Table 6 presents the calculated effective elastic modulus following exposure to fire for 0, 30, 60, and 120 minutes. The calculated results indicate that the effective elastic moduli of beams B_1, B_2, and B_3 were 31.9, 47.9, and 62.5%, respectively, less than those of the reference beam (B).

The moment–area method of determining deflections provides a means of determining the slopes and deflections due to bending in beams and frames. The change in slope between two points on the elastic curve is equal to the area of the M/EI diagram between these points. The deflection curve (differential) equation between support and middle point, loaded as in Figure 10, can be presented as,

$$\frac{\mathrm{d}^2 y}{\mathrm{d}x^2} = \frac{M}{EI} = \frac{57.5P}{EI} \tag{23}$$

where, E and I are the elastic modulus and moment of inertia of the beam section, respectively, and P is the load. The double-integration method involves the double integrals in Equation (23). It is used with the calculation of the integral coefficients from boundary conditions, to yield the deflections as,

$$y = \frac{P}{EI}\left(\frac{57.5}{2}x^2 - 4600x\right) = \frac{P}{EI}(-184{,}000) \tag{24}$$

The maximum deflection of the RC beams after fire exposure can be determined from Equation (24) at the midspan. The calculated load–maximum deflection relations are compared with the test results for beams that had been exposed to fire for 0, 30, 60, and 120 minutes. Figure 14 compares the load–maximum deflection relations of experimental results with calculated data for the reference beam at 30, 60, and 120 minutes, respectively. The slopes of the experimental curve decrease as load increases; however, the slopes are not far from the calculated results. The calculated and experimental results are very similar following fire exposure for 30

Table 6. Calculated effective elastic modulus of beams exposed to fire.

	Beam			
Properties	**B**	**B1**	**B2**	**B3**
Fire exposure time (minutes)	0	30	60	120
Effective elastic modulus (MPa)	21578	14703	11233	8097

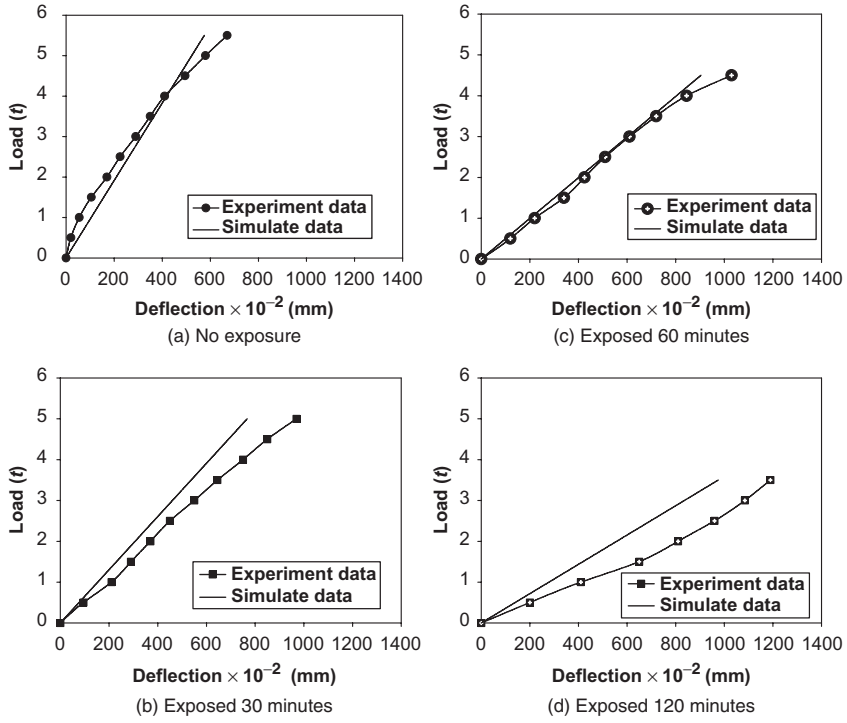

Figure 14. *Comparison between experimental and simulated data with various durations of fire exposure.*

and 60 minutes. The calculated results start to deviate from experimental data after 120 minutes of fire exposure. This result indicates that long-term fire damage may have destroyed the beam structure. The predicted effective elastic moduli of beams exposed to fire for a relatively long period typically exceed the actual values, and the proposed modeling method should be applied conservatively in such cases.

DISCUSSION

To realize the effects of fire on residual mechanical properties and structural performance of RC beams, the study in this article simulated the residual bending moment, shear strength, and elastic modulus of RC beams heated on three surfaces (the tops were insulated) with ASTM E 119 standard temperature-rise curve [18]. The beam cross sections were rectangular at 300 mm wide and 500 mm depth, 4 ϕ 25 steel bars were used for tensile reinforcement, 2 ϕ 25 steel bars as the compressive reinforcement

Table 7. Modeling predictions of the residual values and ratios of bending moment with duration of fire.

	Positive bending moment		Negative bending moment	
Duration of fire (minutes)	**Value (kN m)**	**Ratio (%)**	**Value (kN m)**	**Ratio (%)**
0	306.87	100	160.37	100
20	295.68	96.35	147.14	91.76
40	286.96	93.51	140.41	87.56
60	271.71	88.54	134.94	84.14
80	245.87	80.12	130.44	81.34
100	221.01	72.02	125.43	78.21
120	199.88	65.13	119.73	74.66
140	181.22	59.05	112.51	70.16
160	162.12	52.83	103.73	64.68
180	143.39	46.73	N	N
200	125.18	40.79	N	N
220	108.62	35.39	N	N
240	94.58	30.82	N	N

N means the beam has failed.

and 10 mm steel bar spacing of 100 mm as the shear reinforcement. The compressive strength of the concrete was 2.06×10^7 Pa, and yield strength of the steel bar was 4.12×10^8 Pa.

Table 7 shows the predictions of residual values and ratios of positive and negative bending moments with duration of fire. The bending moment is positive when a beam tends to produce tension under the neutral axis of the beam and compression above the neutral axis; otherwise the bending moment is negative. A beam may sustain a negative bending moment in addition to a positive bending moment during an earthquake. The effects of fire damage on the negative bending moment could be more serious than that on the positive bending moment. Figure 15 plots the residual ratios of positive and negative bending moments with the duration of fire. The residual ratio of positive bending moment declined to 30.82% following exposure to fire for 240 minutes. However, the beam failed in negative bending moment after 173 minutes of fire exposure. Beams that experience positive bending moment merely have a reduction of residual bending moment after fire exposure. In comparison, a beam with a negative bending moment, after exposure to fire, might be crushed by compressive failure once a critical point is exceeded.

The residual shear strengths and ratios, provided by concrete and shear reinforcement, have been predicted in the model discussed in this article. Table 8 presents prediction results. Figure 16 plots the residual ratios of

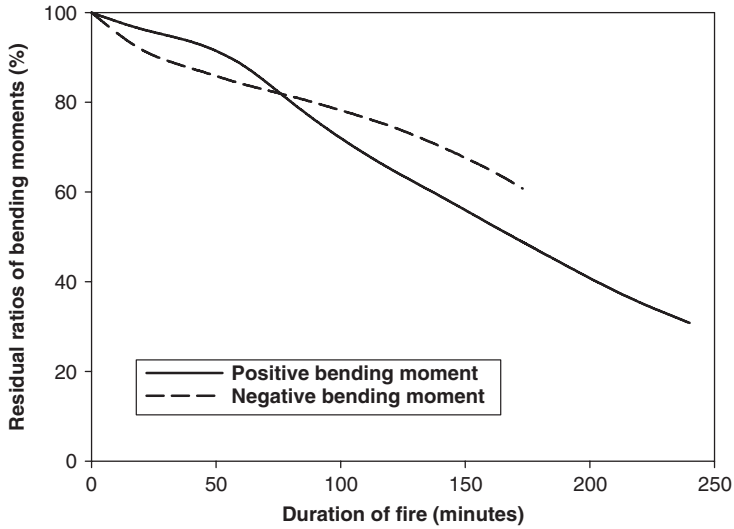

Figure 15. *Residual ratios of positive and negative bending moments as a function of duration of fire exposure.*

shear strength with duration of fire. The residual ratio of the whole shear strength decreased to 29.0% after fire exposure of 240 minutes. The shear strength provided by concrete decreased smoothly from 100%, when first heated, to 64.76% after fire exposure of 240 minutes. The shear strength provided by shear reinforcements remained nearly the same during the first 40 minutes of fire, and decreased quickly when this reinforcement started declining. The shear reinforcement provided the main portion of the total shear strength, and decreased quickly when the yield strength was decreased by high temperature. The concrete covering delayed the influence of high temperature on shear reinforcement. Ensuring that the thickness of concrete covering is adequate is helpful in protecting from fire damage due to reduction of shear strength.

Table 9 displays the predictions of residual values and ratios of elastic modulus. Figure 17 plots the residual ratios of positive (negative) bending moment, shear strength, and elastic modulus with fire duration. All curves have similar tendencies and the residual ratios decreased following fire. The elastic modulus declined significantly at all fire exposure durations. Decreases to shear strength are moderate in the early stages of a fire because of the protection of the concrete covering; however, the shear strength decreased quickly when the shear strength provided by shear reinforcement started declining.

Table 8. Modeling predictions of the residual values and ratios of shear strength with duration of fire.

	Whole shear force (kN)		Provided by concrete (kN)		Provided by stirrups (kN)	
Duration of fire (minutes)	Value (kN)	Ratio (%)	Value (kN)	Ratio (%)	Value (kN)	Ratio (%)
0	352.45	100	102.85	100	249.60	100
20	347.46	98.58	97.94	95.23	249.52	99.97
40	339.66	96.37	92.88	90.31	246.79	98.87
60	315.40	89.49	89.78	87.29	225.63	90.39
80	267.97	76.03	87.15	84.74	180.82	72.44
100	221.51	62.85	84.42	82.08	137.09	54.92
120	186.99	53.05	81.57	79.32	105.41	42.23
140	161.36	45.78	77.93	75.77	83.43	33.43
160	143.81	40.80	75.98	73.87	67.83	27.18
180	130.38	36.99	73.99	71.94	56.39	22.59
200	119.72	33.97	71.97	69.98	47.37	18.98
220	110.85	31.45	69.79	67.86	41.05	16.45
240	102.35	29.04	66.60	64.76	35.75	14.32

Table 9. Modeling predictions of the effective elastic modulus and ratios with duration of fire.

Duration of fire (minutes)	Value (MPa)	Ratio (%)
0	21,281	100
20	16,717	78.56
40	13,822	64.95
60	11,922	56.02
80	10,212	47.99
100	9021	42.39
120	7895	37.10
140	6932	32.57
160	6154	28.92
180	5440	25.56
200	4781	22.46
220	4157	19.54
240	3558	16.72

CONCLUSION

This article presents a novel general analytical model for assessing the effect of fire on the residual mechanical properties

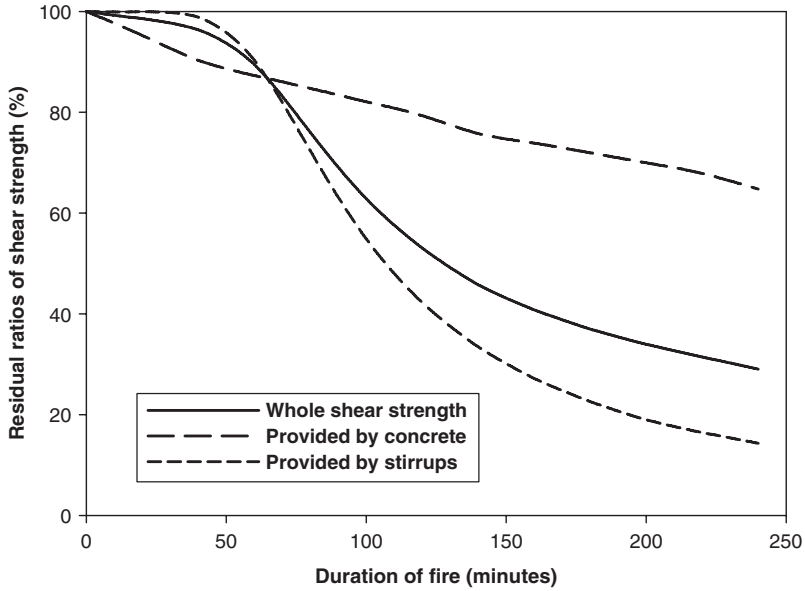

Figure 16. *Residual ratios of shear force as a function of duration of fire exposure.*

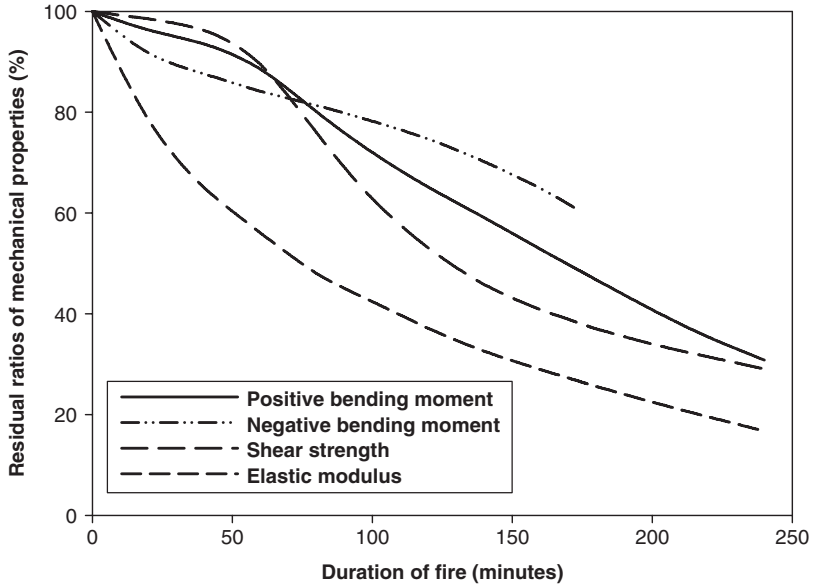

Figure 17. *Residual ratios of bending moment, shear force and elastic modulus as a function of duration of fire exposure.*

and structural performance of RC beams. The following is a list of conclusions:

1. Damage to structures caused by fire need to be carefully evaluated and the behaviors of structures exposed to fire must be modeled. The residual bending moment, shear strength, and elastic modulus of fire-damaged RC beams are successfully characterized by mathematical expressions in this investigation. The modeling results are very helpful to understanding fire resistance and the deformation characteristics of fire-damaged RC beams.
2. The residual bending moment, the shear strength, and the elastic modulus of a RC beam after fire exposure are mathematically modeled and calculated in this study. Modeling results have been compared with full-scale fire exposure experiments. The calculated values based on the model are typically less than the corresponding experimental values, indicating that results are conservative. The values of the predicted residual properties of beams exposed to fire for a relatively long time period typically exceed those of the collected data in experiments. In such cases, the appropriateness of the proposed modeling mechanism should be further investigated.
3. Computational results indicate that bending moment, shear strength, and elastic modulus all progressively decrease as fire duration increases. Furthermore, bending moment, shear strength, and elastic modulus decrease at different rates. As all fires differ, beams may be exposed to distinct fire conditions; consequently, a unified framework to analytically model the residual mechanical properties of fire-damaged RC beams is needed urgently.
4. In full-scale fire tests, no study has investigated flexural failure based on negative bending moment. Based on modeling results, an RC beam with a negative bending moment after exposure to fire can be unexpectedly crushed by compressive failure once a critical point is exceeded. A beam may sustain negative bending moment in addition to positive bending moment during an earthquake. Hence, the safety of fire-damaged RC structures with negative bending moments must be assessed with care in a seismic region.
5. The concrete covering may delay the influence of high temperature on the strength of shear reinforcement. Hence, the thickness of the concrete covering must be adequate to protect against fire damage due to reduction of shear strength.
6. The calculation in the proposed model assumes that a beam section remains complete (no cracking) following fire damage. When cracks are

observed in a beam section after fire damage, the legitimacy of using this model must be evaluated.

FURTHER WORK

The application of this study to real cases revealed the effectiveness and potential of the proposed method. Further research currently underway is studying how different parameters influence an RC beam after fire exposure. Moreover, beams are the main elements in a building's structural system. As no two fires are the same, modeling results in this study will prove helpful when probing how different fires affect building structural systems.

NOMENCLATURE

A_s = area of reinforcing steel
A_v = area of shear reinforcement
B = width of the beam
$c(T)$ = specific heat of the material
c = distance from the extreme compression fiber to the neutral axis
D = effective depth of the beam
f'_c = specified compressive strength of concrete
$f^T_{c,ij}$ = concrete residual compressive stress of lump unit ij after sustaining temperature T and at strain of $\varepsilon_{c,ij}$ ($\varepsilon_{c,ij}$ denotes the strain at the center of each lump unit ij)
f_y = specified yield strength of reinforcement steel
f_{yr} = residual yielding strength of reinforcement steel after sustaining temperature T
$K(T)$ = the thermal conductivity of the material at temperature T
k_{ET} = the ratio of E_T (the modulus of elasticity at elevated temperature) to E (the modulus of elasticity at 20°C)
$K_{y,T}$ = the ratio of f_{yr} (the yield strength at elevated temperature) to f_y (the yield strength at 20°C)
l_n = clear span measured face-to-face of support
M = unitary numbers in beam width
M_u = factored moment forced at section
s = spacing of shear reinforcement in direction parallel to longitudinal reinforcement
T = the highest temperature that the materials have endured

T = time variable
u''' = rate of local heat source per unit volume
V_c = nominal shear strength provided by concrete
V_s = nominal shear strength provided by shear reinforcement
V_u = factored shear forced at section
ρ = ratio of reinforcement
$\gamma(T)$ = density of the material
Δx, Δy = width and depth of lump unit

REFERENCES

1. Gruz, C.R., "Elastic Properties of Concrete at High Temperature," Journal of the PCA Research and Development Laboratories, Vol. 8, No. 1, 1966, pp. 37–45.
2. Smith, E.E. and Harmathy, T.Z., Design of Building for Fire Safety, American Society for Testing and Materials, Philadelphia, 1979.
3. Carman, A.D. and Nelson, R.A., "The Thermal Conductivity and Diffusivity of Concrete," Engineering Experimental Station, University of Illinois, Urbana, Bulletin No. 122, 1921, p. 32.
4. Uddin, T. and Culver, C.G., "Effect of Elevated Temperature on Structure Members," Journal of structural Diversion ASCE 101, 1975, pp. 1531–1549.
5. ACI Committee 216, "Guide for Determining the Fire Endurance of Concrete Elements," ACI 216–81. Concrete Int. 3, 1981, pp. 13–47.
6. Kong, F.K., Evans, R.H., Cohen, E. and Rall, F., Handbook of Structural Concrete, McGraw-Hill, New York, 1983.
7. Lin, T.D., "Measured Temperature in Concrete Beams Exposed to ASTM E 119 Standard Fire," Research and Development Report, Portland Cement Association, Skokie, 1985.
8. Moetaz, M.E., Ahmed, M.R., Ahmed, A.E. and Shadia, E., "Effect of Fire on Flexural Behavior of RC Beams," Construction and Building Materials, Vol. 10, No. 2, 1996, pp. 147–150.
9. Ho, S.W., "A Study of the Mechanical Behavior of Concrete Members after Fire," Master Thesis, National Taiwan Industrial and Technological Institute, Taiwan (1989).
10. Lin, I.J., Chen, S.T. and Lin, C.J. "The Shear Strength of Reinforcing Concrete Beam after Fire Damage," Structure Safety Evaluation after Fire Damage Scientific & Technical Publishing Co., Ltd. Taiwan, 1999, pp. 117–136.
11. Andrew H. Buchanan., Structure Design for Fire Safety. John Wiley & Sons, Ltd, 2000.
12. Harmathy, T.Z., "Thermal Properties of Concrete at Elevated Temperatures," ASTM Journal of Materials, Vol. 5, No. 1, 1970, pp. 47–74.
13. Yunus A. Çengel., Heat Transfer: A Practical Approach, (International Edition), McGraw-Hill, 1998, pp. 57–111.
14. ACI 318R-02, Building Code Requirements for Structural Concrete and Commentary, American Concrete Institute, Michigan, 2002.
15. Eurcode 2 (EC2): Design of Concrete Structures. ENV 1992-1-2: General Rules – Structural Fire Design. European Committee for Standardization, Brussels, Belgium, 1993.
16. Eurcode 3 (EC3): Design of Steel Structures. ENV 1993-1-2: General Rules – Structural Fire Design. European Committee for Standardization, Brussels, Belgium, 1995.

17. Abrams, M.S., ''Compressive Strength of Concrete at Temperature to 1600°F,'' Temperature and Concrete, ACI Publication SP25, 1968, pp. 33–58.
18. Zhao, X.H. and Chen, W.F., ''Effective Elastic Moduli of Concrete with Interface Layer,'' Computers & Structures, Vol. 66, No. 2–3, 1998, pp. 275–288.
19. American Society for Testing and Materials E119–05, Standard Test Methods for Fire Tests of Building Construction and Materials, 2005.